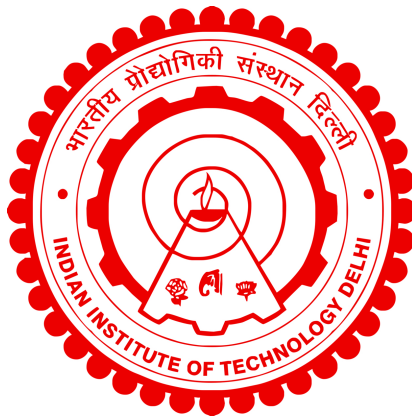


**DEVELOPMENT OF WEAR AND
CORROSION-RESISTANT COATING FOR
STEELS USING THE HVOF THERMAL
SPRAY PROCESS**

ABHIJIT PATTNAYAK



**CENTRE FOR AUTOMOTIVE RESEARCH AND
TRIBOLOGY**

INDIAN INSTITUTE OF TECHNOLOGY DELHI

October 2024

© Indian Institute of Technology Delhi (IITD), New Delhi, 2024

**DEVELOPMENT OF WEAR AND
CORROSION-RESISTANT COATING FOR
STEELS USING THE HVOF THERMAL
SPRAY PROCESS**

by

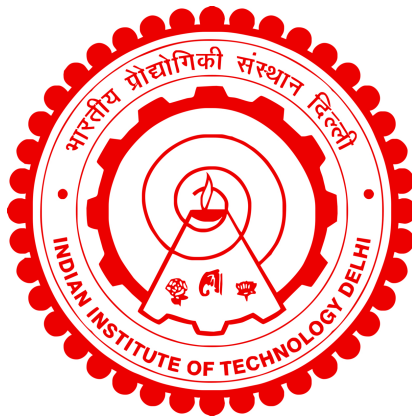
ABHIJIT PATTNAYAK

**CENTRE FOR AUTOMOTIVE RESEARCH AND
TRIBOLOGY**

submitted

in fulfillment of the requirements of the degree of Doctor of Philosophy

to the



INDIAN INSTITUTE OF TECHNOLOGY DELHI

October 2024

Dedicated to my parents

Certificate

This is to certify that the thesis entitled “**Development of wear and corrosion resistant coating for steels using the HVOF thermal spray process**”, submitted by **Mr. Abhijit Pattnayak** to the Indian Institute of Technology Delhi, for the award of the degree of **Doctor of Philosophy** in June 2024, is a record of the original, bonafide research work carried out by him under our supervision and guidance. The thesis has reached the standards fulfilling the requirements of the regulations related to the award of the degree.

The results contained in this thesis have not been submitted in part or in full to any other University or Institute for the award of any degree or diploma to the best of our knowledge.

Dr. Deepak Kumar
Professor
Centre for Automotive
Research and Tribology,
Indian Institute of
Technology Delhi.

Dr. Jayant Jain
Professor
Department of Material
Science and Engineering,
Indian Institute of
Technology Delhi.

Dr. Vijay Chaudhry
Scientific Officer-H
Nuclear Power
Corporation of India
Limited
Department of Atomic
Energy, Mumbai.

Acknowledgements

First of all, I would like to thank the almighty for creating a sense of self-belief in me and blessing me throughout this journey. I am equally thankful to my parents, my brother, and my sister-in-law who provided unconditional support during this journey. I am also grateful to Garima Maurya for her constant motivation and support at every step of my academic journey. I would like to express my profound and heartfelt gratitude to my supervisors (Prof. Deepak Kumar, Prof. Jayant Jain, and Dr. Vijay Chaudhry) for their insightful, invaluable supervision and endless motivation to excel in the present work. Their unique and thought-provoking perspectives towards research and beyond not only developed a scientific temper in me but also boosted my confidence to face any hurdles during this journey.

I thank my SRC members (Prof. S. Fatima, Prof. H. Kanchwala, and Prof. N.N. Gosvami) for their helpful suggestions during the semester's progress presentations. I am also thankful to the Nano Research Facility (NRF) and Central Research Facility (CRF), Indian Institute of Technology Delhi for all the experimental support and timely interventions.

I would like to take this opportunity to express my gratitude to some special friends like Dr. Saroj Kumar Samantaroy, Ms. Krishna Priyadarshini Das, and Dr. Shubhasanket Panda (IIT Kanpur) who became inalienable parts of my Ph.D. journey by providing emotional, mental, and experimental support during this journey.

I appreciate the help and support of our research group Dr. Sanjeet Kumar, Dr. Jaya Gupta, Dr. Harprabhjot Singh, Dr. A.P.S. Lodhi, Dr. Avi Gupta, Dr. Ankit Saxena, Mr. Bharat Kumar, Mr. Abhijith N.V, Ms. Gazal Gupta, And Mr. Arun G. I express my sincere thanks to Dr. Jitendra Narayan Panda, Dr. Umesh Marathe, Late Dr. Meghashree Pradhan, Dr. Bhaskar Bhatt, Dr. Vinay Saini, and Mr. Avtar Singh for helping me in various experiments. I am also thankful to my other colleagues: Dr. Sucharita, Dr. Abinash, Dr. Sreeshan, Dr. Pooja, Harshal, Vikram, Vandana, Sunil, Shravan, Kartikeya, Vishal, Biswajit, Swayam, Sandeep, Chinmay, Subhakar, Rashi, Junaid, Palak, Sunali, Bhavya, Rishmay, and Jonty for their help and support.

Last but the most important ladies of my life are my mother and my M-tech supervisor Dr. Kalyani Mohanta, who always pushed me to make a career in scientific research and provided unconditional support and guidance during my hard times.

Thank you all and may God watch over you.

Abhijit Pattnayak

Abstract

Advanced engineering steels like 17-4 PH steel and ASME SA 387 steel find their applications in critical sectors of the economy like nuclear, chemical, fertilizer, power generation, boilers, pressure vessels, etc. These steels are often used in aggressive environments like high pressure and temperature, and highly corrosive-erosive environments which lead to the premature failure of these steels. For example, 17-4 PH steel exhibits poor tribological properties and fails due to galling in extreme environments. Similarly, SA 387 steel is prone to erosive wear. The improvement in the surface and sub-surface properties of these steels is the most viable solution to prolong their usage in these extreme environmental conditions thereby reducing the material wastage and costs associated with it. Heat treatment can resolve these issues up to some extent, but the problem still persists. Surface coating is another technique to enhance the surface and subsurface properties of a component. Deposition of protective surface coatings especially thermally sprayed ceramic-based coatings has gained significant interest in the past decade due to their excellent anti-wear, anti-corrosion, and high-temperature applications. Among the thermal spray processes, the high-velocity oxy-fuel (HVOF) process has the advantage of developing anti-wear, anti-corrosive, and anti-erosive coatings at relatively low temperatures and high velocity (supersonic) that help in developing a dense coating with better adhesion with the substrate. The current research is aimed at developing hard (anti-wear), anti-corrosive, and anti-erosive ceramic-based coatings using the HVOF process. It has been divided into three modules, namely, the development of reduced graphene oxide (rGO)-doped Al_2O_3 -based coating, exploring the effect of heat treatment on the coating performance, and benchmarking the performance of coated and nitrided 17-4 PH steel. For each module, several characterization techniques were used to investigate the properties of the coating and substrates in detail. For example, the hardness (Vickers and scratch) and tribological responses were recorded using a universal (CETR-UMT) tribometer. The as-coated, flame-treated, and worn surfaces were analyzed using Goniometer, scanning electron microscope (SEM), energy dispersive spectroscopy (EDS), Raman spectroscopy, and 3-D optical profilometer. Corrosive degradation was studied using potentiodynamic polarization and electrical impedance spectroscopy (EIS). Furthermore, the erosion response of the coating was recorded using an air jet erosion test rig at room temperature.

In the case of developing rGO-doped Al₂O₃-based coating on 17-4 PH steel, the addition of rGO into the Al₂O₃-0.8 wt.% CeO₂ matrix enhanced the density of the coating by promoting localized melting due to the high thermal conductivity of the rGO thereby reducing the surface roughness. The improved density in the coating led to improvement in the micro-hardness, nano-hardness, and enhanced corrosion resistance compared to the rGO-less coating. The optimum concentration of rGO was determined to be 0.2 wt.%. This Al₂O₃-0.8 wt.% CeO₂-0.2 wt.% rGO coating outperformed the other coatings and the bare steels in terms of physical, mechanical, tribological, and chemical properties. For example, the elastic modulus and nano-hardness of Al₂O₃-0.8CeO₂-0.2rGO coating were $\approx 101\%$ and $\approx 87\%$ higher than that of Al₂O₃-CeO₂ coating, respectively. The specific wear rate of Al₂O₃-0.8CeO₂-0.2rGO coating was reduced by ≈ 10 times compared to that of 17-4 PH steel at 50 N (379 MPa) load. The improved properties could be attributed to the dense microstructure of the coatings with the introduction of rGO and the participation of rGO in the tribological process. Furthermore, to study the substrate effect on the Al₂O₃-0.8CeO₂-0.2rGO coating and widen the application of this coating, the same composition coating was deposited on SA 387 steel using the HVOF thermal spray process. The properties of the developed coating were then compared with the previously developed same-composition coating on 17-4 PH steel. The results indicated that the coating on SA 387 steel was relatively softer and less corrosion-resistant than the coating on 17-4 PH steel. The reason could be attributed to the presence of diffused iron in the coating on SA 387 steel. Also, the ceramic coating performed better in terms of erosive wear resistance than the SA 387 steel owing to its higher hardness.

The work on exploring the effect of thermal treatment on Al₂O₃-0.8CeO₂-0.2 rGO coating on 17-4 PH steel was planned to access the high-temperature applicability and change in physical, mechanical, and chemical properties of the coating. The heat treatment was done using an oxy-acetylene flame. The results revealed that the thermal treatment severely deteriorated the coating properties. The specific wear rate and corrosion rate of the coating increased by ≈ 165 times and ≈ 1500 times, respectively. This deterioration in the heat-treated coating properties was attributed to the evaporation of the reinforced rGO from the as-sprayed coating making the coating highly porous. So, it is not advisable to heat treat the above-mentioned coating composition above 400 °C.

Finally, a comparative study was carried out to evaluate the performance of the $\text{Al}_2\text{O}_3\text{-}0.8\text{CeO}_2\text{-}0.2$ rGO coating on 17-4 PH steel, the nitrided 17-4 PH (N17-4 PH) steel, and bare 17-4 PH steel. The results showed that nitriding improved the wear resistance of the 17-4 PH steel but reduced its corrosion resistance significantly. Further, the ceramic-based coating performed better than the other two specimens regarding mechanical, tribological, and electrochemical properties. To be specific, the coating was ≈ 10 times and ≈ 6 times more wear-resistant than 17-4 PH steel and N17-4 PH steel, respectively, at 50 N (379 MPa) load. The performance enhancement in the coating was ascribed to the coating hardness, dense microstructure, and introduction of rGO in the coatings, which participated in the tribological process. Further detailed analysis of the specimens' properties reveals that the nitriding process can be replaced with the proposed ceramic-based coating using the HVOF technique for tribological, corrosive, and other applications for 17-4 PH steel.

सारांश

१७ - ४ पीएच स्टील और एएसएमई एसए ३८७ स्टील जैसे उन्नत इंजीनियरिंग स्टील्स का उपयोग अर्थव्यवस्था के महत्वपूर्ण क्षेत्रों जैसे परमाणु, रासायनिक, उर्वरक, बिजली उत्पादन, बॉयलर, दबाव वाहिकाओं आदि में किया जाता है। इन स्टील्स का उपयोग अक्सर उच्च दबाव और तापमान जैसे आक्रामक वातावरण में किया जाता है, और अत्यधिक संक्षारक-क्षरणकारी वातावरण में किया जाता है, जिससे इन स्टील्स की समय से पहले विफलता होती है। उदाहरण के लिए, १७ - ४ पीएच स्टील खराब ट्रिबोलॉजिकल गुणों को प्रदर्शित करता है और चरम वातावरण में आसंजन के कारण विफल हो जाता है। इसी तरह, एसए ३८७ स्टील क्षरणकारी पहनने के लिए प्रवण है। इन स्टील्स की सतह और उप-सतह गुणों में सुधार इन चरम पर्यावरणीय परिस्थितियों में उनके उपयोग को लंबे समय तक बनाए रखने का सबसे व्यवहार्य समाधान है, जिससे सामग्री की बर्बादी और इससे जुड़ी लागत कम हो जाती है। उष्मा उपचार इन मुद्दों को कुछ हद तक हल कर सकता है, लेकिन समस्या अभी भी बनी हुई है। सतह कोटिंग एक घटक की सतह और उप-सतह गुणों को बढ़ाने के लिए एक और तकनीक है। सुरक्षात्मक सतह कोटिंग्स, विशेष रूप से थर्मल स्प्रे किया गया सिरेमिक-आधारित कोटिंग्स के अवक्षेपण ने पिछले दशक में उनके उत्कृष्ट घिसाव प्रतिरोधी, जंग प्रतिरोधी और उच्च तापमान अनुप्रयोगों के कारण महत्वपूर्ण रुचि प्राप्त की है। थर्मल स्प्रे प्रक्रियाओं में, उच्च-वेग ऑक्सी-ईंधन (एचवीओएफ) प्रक्रिया में अपेक्षाकृत कम तापमान और उच्च वेग (सुपरसोनिक) पर घिसाव प्रतिरोधी जंग प्रतिरोधी और कटाव प्रतिरोधी कोटिंग्स विकसित करने का लाभ है जो सबस्ट्रेट के साथ बेहतर आसंजन के साथ एक सघन कोटिंग विकसित करने में मदद करते हैं। वर्तमान अनुसंधान का उद्देश्य एचवीओएफ प्रक्रिया का उपयोग करके कठोर (घिसाव प्रतिरोधी), जंग प्रतिरोधी और कटाव प्रतिरोधी सिरेमिक-आधारित कोटिंग्स विकसित करना है। इसे तीन मॉड्यूल में विभाजित किया गया है, अर्थात्, कम ऑक्सीकरण ग्राफीन ऑक्साइड (आरजीओ)-डोपेड अल्युमिना -आधारित कोटिंग का विकास, कोटिंग प्रदर्शन पर गर्मी उपचार के प्रभाव की खोज, और लेपित और नाइट्राइड १७ - ४ पीएच स्टील के प्रदर्शन का बेंचमार्किंग। प्रत्येक मॉड्यूल के लिए, कोटिंग और सबस्ट्रेट के गुणों की विस्तार से जांच करने के लिए कई लक्षण वर्णन तकनीकों का उपयोग किया गया था। उदाहरण के लिए, कठोरता (विकर्स और खरोंच) और ट्रिबोलॉजिकल प्रतिक्रियाओं को एक सार्वभौमिक (सीईटीआर-यूएमटी) ट्रिबोमीटर का उपयोग करके रिकॉर्ड किया गया था। लेपित, लौ-उपचारित और घिसी हुई सतहों का विश्लेषण गोनियोमीटर, स्कैनिंग इलेक्ट्रॉन माइक्रोस्कोप (एसईएम), ऊर्जा फैलाव स्पेक्ट्रोस्कोपी (ईडीएस), रमन स्पेक्ट्रोस्कोपी और त्रि-डी ऑप्टिकल प्रोफाइलोमीटर का उपयोग करके किया गया था। संक्षारक गिरावट का अध्ययन पोटेंशियोडायनामिक ध्रुवीकरण और विद्युत प्रतिबाधा स्पेक्ट्रोस्कोपी (ईआईएस) का उपयोग करके किया गया था। इसके अलावा, कोटिंग की क्षरण प्रतिक्रिया को कमरे के तापमान पर एक एयर जेट क्षरण परीक्षण रिग का उपयोग करके रिकॉर्ड किया गया था। १७ - ४ पीएच स्टील पर आरजीओ-डोपेड अल्युमिना -आधारित कोटिंग विकसित करने के मामले में, अल्युमिना - ०.८ वजन प्रतिशत सेरिया मैट्रिक्स में आरजीओ को जोड़ने से आरजीओ की उच्च तापीय चालकता के कारण स्थानीयकृत पिघलने को बढ़ावा देकर कोटिंग का घनत्व बढ़ गया, जिससे सतह की खुरदरापन कम हो गई। कोटिंग में बेहतर घनत्व के कारण आरजीओ-रहित कोटिंग की तुलना में माइक्रो-कठोरता, नैनो-कठोरता और संक्षारण प्रतिरोध में सुधार हुआ। आरजीओ की इष्टतम सांद्रता ०.२ वजन प्रतिशत निर्धारित की गई। इस अल्युमिना - ०.८ वजन प्रतिशत सेरिया - ०.२ वजन

प्रतिशत आरजीओ कोटिंग ने भौतिक, यांत्रिक, ट्राइबोलॉजिकल और रासायनिक गुणों के मामले में अन्य कोटिंग्स और नंगे स्टील्स को पीछे छोड़ दिया। उदाहरण के लिए, अल्युमिना - ०.८ सेरिया - ०.२ आरजीओ कोटिंग का लोचदार मापांक और नैनो-कठोरता क्रमशः अल्युमिना - सेरिया कोटिंग की तुलना में $\approx 101\%$ और $\approx 17\%$ अधिक था। ५० न्यूटन (३७९ मेगा पास्कल) लदान पर १७ - ४ पीएच स्टील की तुलना में अल्युमिना - ०.८ सेरिया - ०.२ आरजीओ कोटिंग की विशिष्ट पहनने की दर \square १० गुना कम हो गई थी। बेहतर गुणों को आरजीओ की शुरुआत और ट्रिबोलॉजिकल प्रक्रिया में आरजीओ की भागीदारी के साथ कोटिंग्स के घने माइक्रोस्ट्रक्चर के लिए जिम्मेदार ठहराया जा सकता है। इसके अलावा, अल्युमिना - ०.८ सेरिया - ०.२ आरजीओ कोटिंग पर सबस्ट्रेट प्रभाव का अध्ययन करने और इस कोटिंग के अनुप्रयोग को व्यापक बनाने के लिए, एचवीओएफ थर्मल स्प्रे प्रक्रिया का उपयोग करके एसए ३८७ स्टील पर समान संरचना कोटिंग जमा की गई थी। विकसित कोटिंग के गुणों की तुलना १७ - ४ पीएच स्टील पर पहले से विकसित समान-संरचना कोटिंग से की गई। परिणामों ने संकेत दिया कि एसए ३८७ स्टील पर कोटिंग १७ - ४ पीएच स्टील पर कोटिंग की तुलना में अपेक्षाकृत नरम और कम संक्षारण प्रतिरोधी थी। इसका कारण एसए ३८७ स्टील पर कोटिंग में विसरित लोहे की उपस्थिति को माना जा सकता है। इसके अलावा, सिरेमिक कोटिंग ने एसए ३८७ स्टील की तुलना में क्षरणकारी पहनने के प्रतिरोध के मामले में बेहतर प्रदर्शन किया, क्योंकि इसकी कठोरता अधिक थी।

१७ - ४ पीएच स्टील पर अल्युमिना - ०.८ सेरिया - ०.२ आरजीओ कोटिंग पर थर्मल उपचार के प्रभाव की खोज करने के लिए उच्च तापमान प्रयोज्यता और कोटिंग के भौतिक, यांत्रिक और रासायनिक गुणों में परिवर्तन का पता लगाने की योजना बनाई गई थी। ऑक्सी-एसिटिलीन लौ का उपयोग करके गर्मी उपचार किया गया था। परिणामों से पता चला कि थर्मल उपचार ने कोटिंग के गुणों को गंभीर रूप से खराब कर दिया। कोटिंग की विशिष्ट घिसाव दर और संक्षारण दर लगभग १६५ गुना और लगभग १५०० गुना बढ़ गईं, क्रमशः। गर्मी-उपचारित कोटिंग गुणों में यह गिरावट प्रबलित आरजीओ के वाष्पीकरण के कारण हुई थी, जो छिड़काव किए गए कोटिंग से कोटिंग को अत्यधिक छिद्रपूर्ण बनाता है। इसलिए, ४०० डिग्री सेल्सियस से ऊपर उपर्युक्त कोटिंग संरचना को गर्म करने की सलाह नहीं दी जाती है।

अंत में, १७ - ४ पीएच स्टील, नाइट्राइड १७ - ४ पीएच (एन १७ - ४ पीएच) स्टील और छूछा १७ - ४ पीएच स्टील पर अल्युमिना - ०.८ सेरिया ०.२ आरजीओ कोटिंग के प्रदर्शन का मूल्यांकन करने के लिए एक तुलनात्मक अध्ययन किया गया। परिणामों से पता चला कि नाइट्राइडिंग ने १७ - ४ पीएच स्टील के पहनने के प्रतिरोध में सुधार किया, लेकिन इसके संक्षारण प्रतिरोध को काफी कम कर दिया। इसके अलावा, सिरेमिक-आधारित कोटिंग ने यांत्रिक, ट्राइबोलॉजिकल और इलेक्ट्रोकेमिकल गुणों के संबंध में अन्य दो नमूनों की तुलना में बेहतर प्रदर्शन किया। विशेष रूप से, ५० न्यूटन (३७९ मेगा पास्कल) लोड पर कोटिंग १७ - ४ पीएच स्टील और एन १७ - ४ पीएच स्टील की तुलना में क्रमशः ≈ 10 गुना और ≈ 6 गुना अधिक घिसाव प्रतिरोधी थी। कोटिंग में प्रदर्शन वृद्धि का श्रेय कोटिंग की कठोरता, सघन सूक्ष्म संरचना और कोटिंग्स में आरजीओ की उपस्थिति को दिया गया, जिसने ट्रिबोलॉजिकल प्रक्रिया में भाग लिया। नमूनों के गुणों के आगे विस्तृत विश्लेषण से पता चलता है कि नाइट्राइडिंग प्रक्रिया को १७ - ४ पीएच स्टील के लिए ट्रिबोलॉजिकल, संक्षारक और अन्य अनुप्रयोगों के लिए एचवीओएफ तकनीक का उपयोग करके प्रस्तावित सिरेमिक-आधारित कोटिंग से बदला जा सकता है।

Contents

Certificate

Acknowledgements II

Abstract IV

सारांश

Contents IX

List of Figures XIII

List of Tables XIX

Abbreviations XXI

1	Introduction and literature survey	1
1.1	Introduction	1
1.2	Thermal spray coatings	5
1.3	High-velocity oxy-fuel (HVOF) process	6
1.4	Ceramic-based coatings	7
1.5	Literature review	9
1.5.1	Potential area for coating	10
1.5.2	Characteristics of thermal spray coatings	11
1.6	Motivation	13
1.7	Problem formulation	14
1.7.1	Problem identification	14
1.7.2	Problem definition	15
1.7.3	Research objectives	16
1.7.4	Approach	17

1.8	Thesis outline	18
1.8.1	Chapter 1 Introduction and Literature Survey	18
1.8.2	Chapter 2 Materials and methods	18
1.8.3	Chapter 3 Development of rGO-doped Al ₂ O ₃ -based coating	20
1.8.4	Chapter 4 Effect of heat treatment on the coating performance	20
1.8.5	Chapter 5 Coated and nitrided 17-4 PH steel: A comparative performance evaluation	21
1.8.6	Chapter 6 Conclusions and Future Scope	21
2	Materials and methods	23
2.1	Materials	23
2.2	Coating formulation and post-processing	24
2.3	Coating characterization – Physical	26
2.3.1	Surface roughness measurement	26
2.3.2	Density measurement	27
2.3.3	Surface wettability	27
2.4	Coating characterization - Metallurgical	28
2.4.1	Scanning electron microscopy (SEM)	28
2.4.2	Energy dispersive X-ray spectroscopy (EDS)	28
2.4.3	X-ray diffraction (XRD)	28
2.4.4	Raman spectroscopy	28
2.5	Coating characterization - Mechanical	29
2.5.1	Vickers hardness (HV)	29
2.5.2	Scratch hardness	29
2.5.3	Nanoindentation	30
2.6	Coating characterization - Tribological	31
2.7	Coating characterization - Electrochemical	31
2.8	Thermogravimetric analysis (TGA)	32
2.9	Erosion response evaluation	32
2.10	Fourier transform infrared spectroscopy (FT-IR)	33
3	Development of rGO-doped Al₂O₃ – based coating	35
3.1	Powder characterization	35
3.2	Physical characteristics of coatings	37
3.2.1	Coating thickness	37
3.2.2	Surface roughness of coatings	38
3.2.3	Density of coatings	38
3.2.4	Wettability of the coatings	39
3.3	Metallurgical characteristics	40
3.4	Mechanical characteristics	43
3.4.1	Micro-hardness	43
3.4.2	Scratch hardness response	46

3.4.3	Nano-Indentation response	47
3.5	High-temperature performance of the coatings	48
3.6	Tribological response of the coatings	50
3.6.1	Friction	50
3.6.2	Wear	51
3.7	Corrosion response	54
3.7.1	Modelling of equivalent electrical circuits	55
3.8	Optimising the best coating composition	55
3.9	Study of substrate effect on the optimized coating	58
3.9.1	Surface wettability	59
3.9.2	XRD analysis	59
3.9.3	Hardness response	60
3.9.3.1	Vickers and scratch hardness	60
3.9.3.2	Nanohardness	61
3.9.4	Erosive wear performance	63
3.9.5	Wear mechanism	63
3.9.6	Corrosion response of the specimens	65
3.9.7	Electrochemical equivalent circuits models	66
3.9.8	FT-IR spectroscopy analysis	67
3.9.9	Comparison of coating properties developed on 17-4 PH steel and SA 387 steel	68
3.10	Summary	74
4	Effect of heat treatment on the coating performance	77
4.1	Physical characteristics	78
4.2	Microstructural analysis	79
4.3	Raman spectroscopy	81
4.4	TGA of rGO	82
4.5	Mechanical Characteristics	83
4.5.1	Vickers hardness	83
4.5.2	Scratch hardness	83
4.6	Tribological performance	84
4.7	Corrosion response	86
4.8	Effect of heat treatment on the coating performance	87
4.9	Summary	93
5	Coated and nitrated 17-4 PH steel: A comparative performance evaluation	95
5.1	Physical characteristics	96
5.1.1	Surface roughness measurement	96
5.1.2	Surface wettability	97
5.2	Metallurgical characteristics	97

5.3	Mechanical characteristics	102
5.3.1	Vickers hardness	102
5.3.2	Scratch hardness	103
5.3.3	Nano hardness	104
5.3.4	High-temperature nano hardness	104
5.4	Tribological characteristics	105
5.5	Electrochemical characteristics	107
5.5.1	Equivalent electrical circuits	109
5.6	Comparison between surface nitriding and surface coating	110
5.7	Summary	117
6	Conclusion and future scope	119
6.1	Conclusions	120
6.2	Future scope	122

List of Figures

1.1	Prediction on global steel consumption [1].	2
1.2	Schematic representation of the tribological contact between EN 31 and 17-4 PH steel in nuclear power plant.	3
1.3	Classification of surface coating methods [2].	4
1.4	Principle of the thermal spray process [3]	6
1.5	Comparison among different spray processes in terms of temperature and particle velocity [4].	6
1.6	Schematic representation of the (a) HVOF coating process and (b) developed coating.	7
1.7	Spherical insights ceramic-coating-market reports [5].	9
1.8	Schematic representation of problem formulation and approach for ceramic-based coating development.	17
2.1	Test specimen (a) 17-4 PH steel and (b) OES result of as-received steel.	24
2.2	Schematic representation of the coating development process.	26
3.1	SEM micrographs of (a) alumina, (b) ceria, (c) rGO powder particles, and (d) milled/mixed S ₄ powder.	36
3.2	Particle size distribution data for alumina and ceria.	37
3.3	XRD diffractogram for the powder mixtures S ₁ and S ₄	37
3.4	(a) SEM micrograph to estimate coating thickness of a representative as-sprayed coated sample and (b) average thickness of the as-sprayed coatings.	38
3.5	Average surface roughness of the as-sprayed coatings.	39
3.6	Density of the as-sprayed coatings.	39
3.7	Variation of contact angle of the substrate and different coatings.	40
3.8	Optical and goniometer images of the representative water droplets sitting on (a) 17-4 PH steel and (b) coated sample of composition S ₄ (Al ₂ O ₃ -0.8CeO ₂ -0.2rGO).	40
3.9	SEM micrographs of as-sprayed coatings (a) Al ₂ O ₃ -0.8CeO ₂ , (b) Al ₂ O ₃ -0.8CeO ₂ -0.05rGO, (c) Al ₂ O ₃ -0.8CeO ₂ -0.1 rGO and (d) Al ₂ O ₃ -0.8CeO ₂ -0.2rGO.	41

3.10	SEM micrographs of polished coatings (a) $\text{Al}_2\text{O}_3\text{-}0.8\text{CeO}_2$, (b) $\text{Al}_2\text{O}_3\text{-}0.8\text{CeO}_2\text{-}0.05\text{rGO}$, (c) $\text{Al}_2\text{O}_3\text{-}0.8\text{CeO}_2\text{-}0.1\text{rGO}$ and (d) $\text{Al}_2\text{O}_3\text{-}0.8\text{CeO}_2\text{-}0.2\text{rGO}$	42
3.11	(a) EDS mapping and (b) elemental mapping of as-sprayed S_4 ($\text{Al}_2\text{O}_3\text{-}0.8\text{CeO}_2\text{-}0.2\text{rGO}$) composition sample.	42
3.12	XRD spectrum of S_4 powder and S_4 coated 17-4 steel sample.	44
3.13	Raman spectra of (a) rGO and (b) S_4 ($\text{Al}_2\text{O}_3\text{-}0.8\text{CeO}_2\text{-}0.2\text{rGO}$) coating sample.	44
3.14	Vickers Hardness of the 17-4PH substrate and different coatings.	45
3.15	Representative indentation marks on (a) substrate 17-4 PH, and (b) coated sample S_4	45
3.16	Scratch hardness response of 17-4PH substrate and different coatings.	46
3.17	Representative optical micrographs of scratches made at 50 N load on the (a) 17-4 PH steel and (b) coated sample S_4	47
3.18	P-h curves recorded during nanoindentation made on 17-4 PH steel and different alumina-based coatings (a) on the surface and (b) on the interface of the coatings.	48
3.19	Representative P-h curve recorded during nanoindentation on 17-4 PH steel and developed alumina-based coatings at 300 °C.	49
3.20	Variation of coefficient of friction (COF) values for different coatings and substrates at 10 N load.	51
3.21	Optical micrograph and corresponding RAMAN spectra of the worn surface of S_4 coating.	52
3.22	Wear performance of the samples at various loads.	52
3.23	SEM micrograph of worn surface of (a) 17-4 PH steel and (b) S_4 coating.	53
3.24	(a) and (c) 3D optical profiles and (b) and (d) wear scar profiles of the bare substrate and S_4 coating respectively.	53
3.25	The corrosion response of all the samples where (a) shows the Tafel plots and (b) shows their corrosion rate.	54
3.26	The equivalent electrical circuits modeled for (a) 17-4 PH bare substrate and (b) S_4 coated substrate.	56
3.27	Average contact angle of the specimens and goniometer images of their representative water droplets.	60
3.28	XRD spectrum of (a) bare 17-4 PH steel, (b) bare SA 387 steel, and coatings deposited on (c) 17-4 PH steel and (d) SA 387 steel respectively.	61
3.29	Vickers and scratch hardness of all specimens.	62
3.30	Load (P) vs. displacement (h) curves for (a) bulk specimen surfaces and (b) substrate-coating interface.	62
3.31	The erosive wear performance of SA 387 steel and the coated SA 387 steel.	64
3.32	The erosive wear performance of SA 387 steel and the coated SA 387 steel.	64

3.33	SEM micrographs of the wear regime of (a,b) SA 387 steel and (c,d) the coating.	65
3.34	(a) Tafel plot for the specimens and (b) their corresponding corrosion rates.	66
3.35	Equivalent electrical diagrams containing corrosion impedance of (a) 17-4 PH steel, (b) coating 17-4 PH, (c) SA 387 steel, and (d) coating SA 387.	68
3.36	FT-IR spectra of the coating deposited on SA 387 steel after corrosion test.	69
3.37	Thermal image of the bare SA 387 steel during coating deposition.	70
3.38	Variation of H-E ratios between SA 387 steel and the coating.	71
3.39	(a) SEM micrograph of the corroded SA 387 coating and (b-e) its corresponding elemental mapping.	72
3.40	The schematic representation of the corrosion mechanism in SA 387 coating.	73
3.41	SEM micrographs of the corroded SA 387 coating.	74
3.42	Back-scattered micrographs of the corroded SA 387 coating highlighting intra-splat corrosion.	74
4.1	Density variation and thickness reduction (after polishing) of the coatings before and after post-treatment.	79
4.2	Wettability of different substrates.	79
4.3	SEM micrographs of (a) as-sprayed and (b-c) post-processed coatings.	80
4.4	Enter(a) EDS mapping and (b-d) elemental mapping of PP coating.	81
4.5	Raman spectra of AS and PP coatings.	82
4.6	Thermal degradation behavior of rGO.	82
4.7	(a) Vickers hardness and (b) scratch hardness response of all specimens.	84
4.8	(a) Variation of coefficient of friction (COF) with time for bare 17-4 PH steel, AS, and PP coatings at 10 N load and (b) specific wear rate for different substrates at 50 N load.	85
4.9	3-D optical profiles of worn surfaces (a-c) and corresponding wear depth profiles of different substrates (d-f).	85
4.10	(a) Tafel plot of the specimens and (b) their corresponding corrosion rates.	87
4.11	EIS data-based modeled equivalent electrical circuit for (a) as sprayed, (b) post-processed, and (c) 17-4 PH steel.	87
4.12	SEM micrographs of (a) wear crater of the PP coating, (b) coating-substrate regime, and (c-d) dominant wear modes.	89
4.13	Optical images of corroded (a) the as-sprayed and (b) the post-processed coatings highlighting RDZ.	90
4.14	(a) Optical micrograph and (b) the Raman spectrum of the corroded PP coating.	91

4.15	(a) SEM micrograph of the corroded region of the PP coating and (b-e) its corresponding elemental mapping.	91
4.16	(a) SEM and (b) backscattered micrographs of the corroded PP coating.	92
4.17	Nyquist plot of (a) all the substrates, (b) 17-4 PH steel, and (c) the post-processed coating.	92
4.18	Bode plots for different substrates	93
5.1	(a-c) Representative 2D surface profiles and (d-f) the corresponding 3D surface profiles of the as-received 17-4 PH steel, as-nitrided 17-4 PH, and as-sprayed coating, respectively.	97
5.2	Variation in the contact angles and live images of the water drop on the various specimens during the experiment.	98
5.3	(a) EDS mapping and (b-e) elemental mapping of the as-received 17-4 PH steel.	99
5.4	XRD analysis of 17-4 PH steel.	99
5.5	(a) EDS mapping and (b-f) elemental mapping of the as-received 17-4 PH steel.	100
5.6	XRD spectra of N17-4 PH steel.	101
5.7	Cross-sectional SEM micrographs of (a) as-nitrided 17-4PH steel and (b) as-sprayed ceramic coating.	101
5.8	(a) Vickers hardness of each specimen as well as representative microscopic images of the indents created on (b) 17-4PH steel, (c) N17-4PH steel, and (d) coated specimen.	102
5.9	(a) Scratch hardness of all the specimens and corresponding microscopic images of the scratches made on (b) 17-4PH steel, (c) N17-4PH steel, and (d) coated specimen.	103
5.10	(a) Load (P) vs. displacement (h) curve for all the specimens and (b) their mechanical properties observed during nanoindentation test at room temperature.	104
5.11	Representative load (P) vs. displacement (h) curve for different specimens recorded using nanoindentation (a) and their mechanical properties observed during nanoindentation test at 300°C (b).	105
5.12	(a) Coefficient of friction (COF) variation with time and (b) average COF values for all the specimens when tested under 10 N load at room temperature.	106
5.13	Specific wear rate of the specimens at various loads.	107
5.14	(a-c) Wear scar profiles and (d-f) their corresponding wear scar depths of 17-4 PH steel, N17-4 PH steel, and the coating, respectively.	108
5.15	(a) Tafel curves and (b) corrosion rate for all three substrates.	108
5.16	The modeled electrical circuits for (a) 17-4 PH, (b) N17-4 PH, and (c) coated substrates.	110
5.17	Schematic representation of the scratch hardness mechanism.	113
5.18	H-E ratios for different specimens at room temperature.	114

5.19 SEM micrographs of worn surfaces (a) 17-4 PH steel, (b) N17-4 PH steel, and (c) coating.	115
5.20 Nyquist plot for (a) all specimens, (b) 17-4 PH steel, and (c) N17-4 PH steel, respectively.	116
5.21 Bode plots for all specimens regarding magnitude and phase vs. frequency.	117

List of Tables

1.1	Composition of various steels	11
2.1	Coating feedstock powders nomenclature and their composition	25
2.2	HVOF thermal spraying Parameters	26
2.3	Erosion test parameters	32
3.1	Mechanical properties of 17-4 PH steel and developed alumina-based coatings	47
3.2	Mechanical properties of the coating-substrate interfacial regimes of the developed alumina-based coatings	48
3.3	Mechanical properties of 17-4 PH steel and developed alumina-based coatings at 300 °C	49
3.4	Relative comparison between hardness and elastic modulus values at room temperature (RT) and high temperature (HT)	49
3.5	Hardness and Elastic modulus values of all the specimens in different regions	62
3.6	Charge transfer resistance values (R) for various specimens	67
5.1	Elemental composition of the 17-4 PH steel	98
5.2	Elemental composition of the N17-4PH steel	99
5.3	Charge transfer resistance values for different specimens	109

Abbreviations

rGO	R educed G raphene O xide
HVOF	H igh V elocity O xygen F uel
CGS	C old G as S pray
APS	A tmospheric P lasma S pray
COF	C oefficient of F riction
HV	V ickers H ardness
HS	S cratch H ardness
EIS	E lectrochemical I mpedance S pectroscopy
AS	A s S prayed
PP	P ost P rocessed
PH	P recipitation H ardened
TGA	T hermogravimetric A nalysis
SEM	S canning E lectron M icroscopy
EDS	E nergy D ispersive S pectroscopy
XRD	X -ray D iffraction